

SOLUTION OF FRACTIONAL-ORDER REACTION-ADVECTION-DIFFUSION EQUATION ARISING IN POROUS MEDIA

Chetna Biswas,^{1,*} Subir Das,¹ Anup Singh,² & Manish Chopra³

¹Department of Mathematical Sciences, Indian Institute of Technology (BHU), Varanasi, 221005, India

²Department of Mathematics, Institute of Technology, Nirma University, Ahmedabad-382481, Gujarat, India

³Radiation Safety Systems Division, Bhabha Atomic Research Centre, Mumbai 400085, India

*Address all correspondence to: Chetna Biswas, Department of Mathematical Sciences, Indian Institute of Technology (BHU), Varanasi, 221005, India, E-mail: chetnabiswas.rs.mat19@itbhu.ac.in

Original Manuscript Submitted: 3/2/2022; Final Draft Received: 6/2/2022

In this article, the fractional-order nonlinear reaction-advection-diffusion equation describing contaminant transport in groundwater has been solved using shifted Legendre collocation method. The shifted Legendre polynomial is used to approximate the function. After that the operational matrix for fractional-order derivative in Caputo sense is applied on it. The shifted Legendre collocation points are employed to obtain a system of nonlinear algebraic equations which have been solved using Newton method. The application of the said methodology is demonstrated by applying it to two standard cases. The proposed method is validated by comparing the numerical results with those obtained using exact solutions through error analyses and the results are given in graphical as well as tabular forms. After the validation of its efficiency and effectiveness, the proposed numerical scheme is applied on a mathematical model related to porous media in a fractional order system. The salient feature of this article is the graphical exhibitions of the effects of fractional-order spatial and time derivatives, and also reaction and advection terms on the solution profile for different particular cases.

KEY WORDS: collocation method, fractional-order derivative, Legendre polynomial, operational matrices, Caputo derivative, damping

1. INTRODUCTION

We understand a porous medium as a physical system with voids. These pores are generally filled with fluids like gases or liquids. Porous media is a very useful concept in several areas of applied sciences like filtration, geomechanics, construction, material sciences, etc. By porous media we mean a solid which allows a passage of fluids through its voids and pores. Natural examples of porous media are sand, limestone, etc. Based on structure, porous media can be further characterized at two different geological levels, i.e., microscopic level and macroscopic level. The former deals with the expression of structure with the help of degree of interconnection, orientation of pores, etc. whereas the latter deals with bulk parameters, which have been averaged over scales much larger than the size of pores. Based on our objective, we can prefer any of the two approaches, but to have a basic understanding of surface phenomena such as absorption, it is clear that microscopic description is necessary. Several articles are available in the literature which discuss different models on porous media (Ahmed and Rashed, 2021; Bhrawy and Baleanu, 2013; Chen et al., 2010; Cui, 2015; Davarzani et al., 2021; Ngondiep, 2022; Qawasmeh et al., 2021; Sohail et al., 2021; Wang et al., 2021).

In most cases, pollutant movement in the subsurface is dominated by advection. It describes the pollutant transfer by the bulk movement of flowing groundwater. The movement of mass entrained in the flow is referred to as advection. Solute advection is the movement of dissolved substances due to the movement of the water in which they are suspended. Advection not only moves mass from one place to another, but it also distributes or scatters the matter. This happens because the distribution of water velocity is not uniform. The advection diffusion equation describes the transport of a solute under the combined effects of advection and diffusion. If the chemical being carried through soil is reactive, its behavior in groundwater is described by a reaction-advection-diffusion equation (RADE). The reaction term represents the source and the sink term in the advection-diffusion equation. The additional source term will increase whereas the sink term will lead to reduction in contaminant concentration. Reduction due to degradation will be zero for the case of conservative contaminant.

A groundwater system or aquifer is a classical example of porous media. Contamination of groundwater is a severe problem for humans because its decontamination is an extremely difficult and costly affair. The near-surface or subsurface storage or disposal of waste such as septic tank sludge, grass waste, and industrial wastes is the primary cause of groundwater pollution. When the contaminants enter the aquatic subsurface environment, they move through an aquifer along with groundwater. The fate of the contaminant in natural systems like dust pollution, river thermal pollution, and groundwater contamination may be modeled using a partial differential equation (PDE) and more particularly, a fractional-order PDE (FPDE) (Das, 2009; Das et al., 2011; Singh et al., 2019). The movement of pollutants in the groundwater, atmosphere, and surface water can be more accurately modeled mathematically by the fractional-order reaction-advection-diffusion equation (FRADE).

The spatial and temporal profiles of pollutant concentration in the aquifer can be predicted by solving RADE with defined boundary and initial conditions. Because of numerous applications in diverse domains, such as physical, chemical, geological, biological, and financial systems, fractional calculus has received a lot of attention in recent years. A fractional-order diffusion mathematical model that describes nondiffusive transportation in turbulence of plasma (Del-Castillo-Negrete et al., 2005) and a nonlinear fractional-order diffusion model for the flow in capillaries across porous media are just a few examples (Gerolymatou et al., 2006). The mathematical models of physical systems have been observed to be more precise when fractional calculus is used. In both industry and academia, the use of the fractional derivative as a tool to construct more stable mathematical models to study the complicated engineering problems is gaining popularity. When fractional-order derivatives are used instead of integer-order derivatives, a practical mathematical description of any physical phenomenon based on current and earlier time is produced. The microscopic dynamics of transportation of mass in porous media is extremely complicated, and the physical events have peculiar kinetics that the ordinary diffusion equation cannot account for, but the fractional diffusion equation does.

For contaminant transport in groundwater, fractional-order ADE has shown great prospects in simulating the physical system in a better way as compared to integral order ADE. It has been reported by many researchers that the FRADEs are much more effective than integer order RADEs in simulating the flow and transport in porous media (Ghazal and Behrouz, 2018; Płociniczak, 2015; Zhou and Yang, 2018). For instance, Ghazal and Behrouz (2018) by comparison with observations concluded that for heterogeneous porous media, FRADEs give more accurate results, especially for longer transport distances. Moreover, FRADEs simulated the tailing parts of breakthrough curves much better and accounted for the earlier arrival of tracer. Similarly, Płociniczak (2015) observed better matching of the results of their time fractional RADE with the experimental outcomes. El-Amin (2021) opined that the fractional mass conservation equation can represent the nonlinear flux with more accuracy than the first-order linear Taylor series to account for the related heterogeneity.

The common removal mechanisms in groundwater systems include the presence of microorganisms capable of biodegrading certain compounds, physical decay, and adsorption of the contaminant on the soil part of the aquifer. Biodegradation, an important aspect of contaminant flow, may be enhanced to remove contaminants. Adsorption, a retardation reaction between solute and surface of the porous structure, is an important factor in contaminant movement. Its effects in segregating the hazardous compounds from the groundwater and also slowing the movement of the compound are remarkable. Solute transport phenomena with nonlinear biodegradation occur in many situations like contamination of inorganic chemical and metal in soil and groundwater systems (Karapanagioti et al., 2001; Lee et al., 2021). The contaminant under the condition of nonlinear degradation results into nonlinear differential

equation in both integer-order and fractional-order systems as described in the following mathematical model.

As shown in Benson et al. (2000a) and Benson et al. (2000b), for contaminant migration in heterogeneous porous media and earth surfaces such as natural rivers, the fractional-order form of the RADE is advantageous. To solve the fractional-order transport equation in disordered semiconductors, fractional-order transport equation within Liouville equations is examined by Tarasov (2006). Many scholars have contributed to the development of strategies for solving fractional-order PDEs that are both reliable and efficient. In Jaiswal et al. (2018), a space fractional-order solute transport system is solved using finite difference method. The fractional-order convection–diffusion equation arising in underground water pollution is solved using dual Bernstein operators in Sayevand et al. (2022). In Atangana and Baleanu (2017), the Caputo–Fabrizio derivative is applied to groundwater flow within the confined aquifer. In this article, the following fractional-order nonlinear RADE is considered:

$$\frac{\partial^\alpha c}{\partial t^\alpha} = D \frac{\partial^{2\beta} c}{\partial x^{2\beta}} + D \frac{\partial^{2\beta} c}{\partial y^{2\beta}} - \nu_1 \frac{\partial^\beta c}{\partial x^\beta} - \nu_2 \frac{\partial^\beta c}{\partial y^\beta} - \lambda c(1 - c), \quad (1)$$

where $0 < \alpha \leq 1$, $0.5 < \beta \leq 1$, with the initial condition

$$c(x, y, 0) = \Psi_1(x, y), \quad (2)$$

and boundary conditions

$$c(0, y, t) = \Psi_2(y, t), \quad (3)$$

$$\frac{\partial^\beta c(1, y, t)}{\partial x^\beta} = \Psi_3(y, t), \quad (4)$$

$$\frac{\partial^\beta c(x, 0, t)}{\partial y^\beta} = \Psi_4(x, t), \quad (5)$$

$$\frac{\partial c(x, 1, t)}{\partial y} = \Psi_5(x, t), \quad (6)$$

where c is the function $c(x, y, t) \in C[0, 1] \times C[0, 1] \times C[0, 1]$; D is the diffusion coefficient; and ν_1 and ν_2 are the velocities of solute transport. $\partial^\alpha c / \partial t^\alpha$, $\partial^{2\beta} c / \partial x^{2\beta}$, $\partial^{2\beta} c / \partial y^{2\beta}$, $\partial^\beta c / \partial x^\beta$, and $\partial^\beta c / \partial y^\beta$ are all Caputo fractional-order derivatives of $c(x, y, t)$. Because exact solutions of nonlinear FPDEs are difficult to obtain, the numerical and approximate approaches are used to solve these equations. As discussed previously, numerical solutions utilizing various advanced techniques are beneficial in dealing with nonlinear situations. Since Legendre polynomials satisfy the orthogonality criterion, the Legendre collocation method with operational matrices is a trustworthy method for solving nonlinear FPDEs. During the solution of differential equations, the approach employs a truncated orthogonal series. Legendre operational matrices have been generalized to fractional-order derivative by Saadatmandi and Dehghan (2010).

The following is the arrangement of the article's structure. The preliminary information related to the shifted Legendre approximation and operational matrices are presented in Section 2. Section 3 presents the validation of the mathematical model through two numerical examples. Section 4 contains the solution of the concerned mathematical equation under prescribed initial and boundary conditions and numerical findings. In Section 5, the work is concluded in brief.

2. PRELIMINARY INFORMATION

2.1 Approximation of a Function Using Shifted Legendre Polynomial

Legendre polynomials on $[-1, 1]$ interval are defined by recursive relations as follows:

$$l_0(x) = 0,$$

$$l_1(x) = x,$$

$$l_{m+1}(x) = \frac{2m+1}{m+1}xl_m(x) - \frac{m}{m+1}l_{m-1}(x), \quad m = 1, 2, 3, \dots$$

A Legendre polynomial can be transformed to a shifted Legendre polynomial by using the transformation $t = (x + 1)/2$, and as a result the interval $[-1, 1]$ will be transformed to $[0, 1]$ and the shifted Legendre polynomial becomes

$$L_m(t) = \sum_{k=0}^m (-1)^{m+k} \frac{(m+k)!}{(m-k)! (k!)^2} t^k, \quad m = 0, 1, 2, \dots$$

2.1.1 One-Dimensional Space

The orthogonality condition of shifted Legendre polynomials $L_n(x)$ in one dimension is

$$\int_0^1 L_i(x)L_j(x)dx = \begin{cases} \frac{1}{2i+1} & \text{if } i = j \\ 0 & \text{otherwise.} \end{cases}$$

Consider a function $c(x) \in C[0, 1]$, which is approximated as (Singh and Das, 2019)

$$c(x) \approx \sum_{k=0}^n a_k L_k(x), \quad (7)$$

where

$$a_k = (2k+1) \int_0^1 u(x)L_k(x)dx.$$

This approximation of $c(x)$ in matrix notation will be

$$c(x) \approx A^T \psi(x),$$

where matrix $\psi(x)$ of order $(n+1) \times 1$ and the coefficient matrix A of order $(n+1) \times 1$ are defined as

$$\psi(x) = [L_0(x), L_1(x), L_2(x), \dots, L_n(x)]^T,$$

$$A = [a_0, a_1, a_2, \dots, a_n]^T.$$

2.1.2 Two-Dimensional Space

Similarly, to extend the approximation in two-dimensional space, the shifted Legendre polynomial of order $(n+1)$ can be written as

$$L_m(x, y) = L_i(x)L_j(y),$$

where $m = (n+1)i + j + 1$ and $i = 0, 1, 2, \dots, n, j = 0, 1, 2, \dots, n$.

Here, the orthogonality condition for $L_m(x, y)$ is

$$\int_0^1 \int_0^1 L_{i_1}(x)L_{j_1}(y)L_{i_2}(x)L_{j_2}(y)dx dy = \begin{cases} \frac{1}{(2i_1+1)(2j_1+1)}, & \text{if } i_1 = i_2, \quad j_1 = j_2, \\ 0, & \text{otherwise.} \end{cases}$$

A function $c(x, y) \in C[0, 1] \times C[0, 1]$ can be approximated as (Singh and Das, 2019)

$$c(x, y) \approx \sum_{k=0}^{(n+1)^2} b_k L_k(x, y) = B(\psi_n(x) \otimes \psi_n(y)), \quad (8)$$

where B is the coefficient matrix of order $1 \times (n + 1)^2$ and $\psi_n(x) \otimes \psi_n(y)$ is the Kronecker product of matrices $\psi_n(x)$ and $\psi_n(y)$ of order $(n + 1)^2 \times 1$ defined as

$$\begin{aligned} \psi_n(x) \otimes \psi_n(y) &= [L_0(x)L_0(y), \dots, L_0(x)L_n(y), L_1(x)L_0(y), \dots, L_1(x)L_n(y), \dots, L_n(x)L_0(y), \dots, \\ &L_n(x)L_n(y)]^T, \end{aligned} \tag{9}$$

and

$$B = [b_0, b_1, b_2, \dots, b_{(n+1)^2}]^T.$$

The properties of the Kronecker product and its applications can be found in Brewer (1978) and Zhang and Ding (2013).

2.1.3 (2+1)-Dimensional Space

Using the preceding definitions we can extend approximation in (2+1)-dimensional space. Here, the orthogonality condition for the shifted Legendre polynomial is

$$\begin{aligned} &\int_0^1 \int_0^1 \int_0^1 L_{i_1}(x)L_{j_1}(y)L_{k_1}(t)L_{i_2}(x)L_{j_2}(y)L_{k_2}(t) dx dy dt \\ &= \begin{cases} \frac{1}{(2i_1 + 1)(2j_1 + 1)(2k_1 + 1)}, & \text{if } i_1 = i_2, \quad j_1 = j_2, \\ & k_1 = k_2, \\ 0, & \text{otherwise.} \end{cases} \end{aligned} \tag{10}$$

A function $c(x, y, t) \in C[0, 1] \times C[0, 1] \times C[0, 1]$ can be approximated as (Singh and Das, 2019)

$$c(x, y, t) \approx c_{n,n,n}(x, y, t) = \sum_{i,j,k=0}^n c_{i,j,k} L_{i,j,k}(x, y, t) = (\psi_n(t))^T C(\psi_n(x) \otimes \psi_n(y)), \tag{11}$$

where C is the coefficient matrix of order $(n + 1) \times (n + 1)^2$, $\psi_n(x)$ and $\psi_n(y)$ are matrices both of order $(n + 1) \times 1$, and $(\psi_n(x) \otimes \psi_n(y))$ is the Kronecker product of matrices $\psi_n(x)$ and $\psi_n(y)$ of order $(n + 1)^2 \times 1$, defined as

$$\psi_n(x) \otimes \psi_n(y) = [L_0(x)L_0(y), \dots, L_0(x)L_n(y), L_1(x)L_0(y), \dots, L_1(x)L_n(y), \dots, L_n(x)L_0(y), \dots, L_n(x)L_n(y)]^T.$$

2.2 Operational Matrices

In this section, we will define an operational matrix of a shifted Legendre fractional-ordered derivative of the vector $\psi_n(x)$ as $\frac{\partial^\gamma \psi_n(x)}{\partial x^\gamma} \approx D^{(\gamma)} \psi_n(x)$, where $D^{(\gamma)}$ is given as follows (Saadatmandi and Dehghan, 2010):

$$D^{(\gamma)} = \begin{pmatrix} 0 & 0 & \dots & 0 \\ \vdots & \vdots & & \vdots \\ 0 & 0 & \dots & 0 \\ \sum_{k=\lceil \gamma \rceil}^{\lceil \gamma \rceil} \zeta_{\lceil \gamma \rceil,0,k} & \sum_{k=\lceil \gamma \rceil}^{\lceil \gamma \rceil} \zeta_{\lceil \gamma \rceil,1,k} & \dots & \sum_{k=\lceil \gamma \rceil}^{\lceil \gamma \rceil} \zeta_{\lceil \gamma \rceil,n,k} \\ \vdots & \vdots & & \vdots \\ \sum_{k=\lceil \gamma \rceil}^i \zeta_{i,0,k} & \sum_{k=\lceil \gamma \rceil}^i \zeta_{i,1,k} & \dots & \sum_{k=\lceil \gamma \rceil}^i \zeta_{i,n,k} \\ \vdots & \vdots & & \vdots \\ \sum_{k=\lceil \gamma \rceil}^n \zeta_{n,0,k} & \sum_{k=\lceil \gamma \rceil}^n \zeta_{n,1,k} & \dots & \sum_{k=\lceil \gamma \rceil}^n \zeta_{n,n,k} \end{pmatrix}, \tag{12}$$

where

$$\zeta_{i,j,k} = \frac{2j+1}{h^k} \sum_{p=0}^j \frac{(-1)^{i+p+j+k} (k+i)! (p+j)!}{k!(i-k)! \Gamma(k-\gamma+1) (j-p)! (p!)^2 (k+p-\gamma+1)}.$$

The first $[\gamma]$ rows of $D^{(\gamma)}$ are zero.

Using the preceding definition and results of the article by Brewer (1978), we can compute the fractional partial order derivative of order $\gamma > 0$ of Kronecker product $\psi_n(x) \otimes \psi_n(y)$ with respect to x , as follows:

$$\begin{aligned} \frac{\partial^\gamma}{\partial x^\gamma} (\psi_n(x) \otimes \psi_n(y)) &= \frac{\partial^\gamma \psi_n(x)}{\partial x^\gamma} \otimes \psi_n(y) + \psi_n(x) \otimes \frac{\partial^\gamma \psi_n(y)}{\partial x^\gamma}, \\ &= \frac{\partial^\gamma \psi_n(x)}{\partial x^\gamma} \otimes \psi_n(y) \\ &\approx (D^{(\gamma)} \psi_n(x)) \otimes (I \psi_n(y)) \\ &\approx (D^{(\gamma)} \otimes I) (\psi_n(x) \otimes \psi_n(y)), \end{aligned} \quad (13)$$

and similarly fractional derivative with respect to y gives

$$\frac{\partial^\gamma}{\partial y^\gamma} (\psi_n(x) \otimes \psi_n(y)) \approx (I \otimes D^{(\gamma)}) (\psi_n(x) \otimes \psi_n(y)), \quad (15)$$

where I is the identity matrix and $D^{(\gamma)}$ is operational matrix of fractional-order derivative, and both the matrices are of order $(n+1) \times (n+1)$.

Figure 1 shows the comparison of the Caputo fractional-order derivative of the function $f(x) = x^{2.2}$ when computed directly using the formula and when computed using the operational matrix of the Caputo fractional-order derivative given in Eq. (12).

3. NUMERICAL APPLICATION

This section deals with the validation of the proposed method by applying it to two standard test cases where exact solutions are known. For the comparison of the approximate and the exact solutions, let us define the L^2 error in $0 \leq x \leq 1$ as

$$\|c(x, 1, 1) - c_{n,n,n}(x, 1, 1)\|_2 = \sqrt{\int_0^1 |c(x, 1, 1) - c_{n,n,n}(x, 1, 1)|^2 dx}, \quad (16)$$

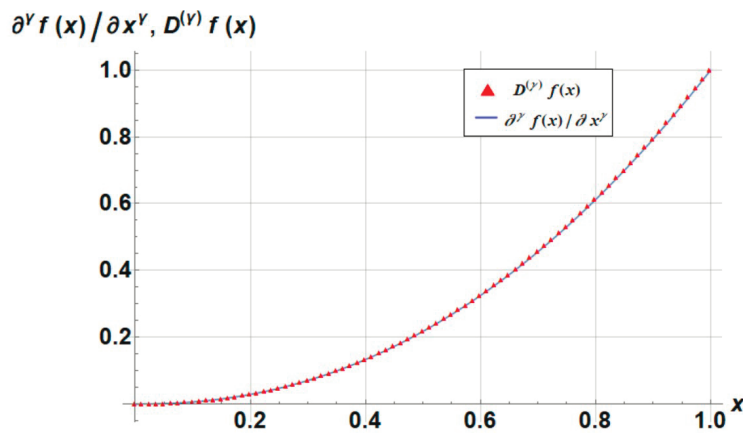


FIG. 1: Plots of comparison between exact and approximate values of Caputo fractional-order derivative for $f(x) = x^{2.2}$ at $\alpha = 0.7$

where $c(x, y, t)$ and $c_{n,n,n}(x, y, t)$ represent the exact and approximate solutions, respectively.

The rate of convergence (ρ) is calculated using the formula

$$\rho = \lim_{k \rightarrow \infty} \frac{\|c_{k+1,k+1,k+1}(x, 1, 1) - c(x, 1, 1)\|_2}{\|c_{k,k,k}(x, 1, 1) - c(x, 1, 1)\|_2}. \tag{17}$$

The L^∞ error in $0 \leq x \leq 1$ is defined as

$$\|c(x, 1, 1) - c_{n,n,n}(x, 1, 1)\|_\infty = \text{Sup}\{|c(x, 1, 1) - c_{n,n,n}(x, 1, 1)| : x \in [0, 1]\}. \tag{18}$$

Example 1. Let us consider the following fractional-order RADE (Singh et al., 2022)

$$\frac{\partial^\alpha c}{\partial t^\alpha} = D \left(\frac{\partial^\beta c}{\partial x^\beta} + \frac{\partial^\beta c}{\partial y^\beta} \right) - v \left(\frac{\partial c}{\partial x} + \frac{\partial c}{\partial y} \right) - \lambda c(1 - c), \quad 0 < \alpha < 1, \quad 1 < \beta < 2, \tag{19}$$

where c is a function in $c(x, y, t) \in C[0, 1] \times C[0, 1] \times C[0, 1]$ with initial condition

$$c(x, y, 0) = \left(1 + \exp \left(\frac{1}{\sqrt{6}} \left(x - \frac{y}{\sqrt{2}} \right) \right) \right)^{-2}, \tag{20}$$

and boundary conditions

$$c(0, y, t) = \left(1 + \exp \left(\frac{1}{\sqrt{6}} \left(-\frac{y}{\sqrt{2}} \right) - \frac{5t}{\sqrt{6}} \right) \right)^{-2}, \tag{21}$$

$$c(1, y, t) = \left(1 + \exp \left(\frac{1}{\sqrt{6}} \left(1 - \frac{y}{\sqrt{2}} \right) - \frac{5t}{\sqrt{6}} \right) \right)^{-2}, \tag{22}$$

$$c(x, 0, t) = \left(1 + \exp \left(\frac{1}{\sqrt{6}} (x) - \frac{5t}{\sqrt{6}} \right) \right)^{-2}, \tag{23}$$

$$c(x, 1, t) = \left(1 + \exp \left(\frac{1}{\sqrt{6}} \left(x - \frac{1}{\sqrt{2}} \right) - \frac{5t}{\sqrt{6}} \right) \right)^{-2}, \tag{24}$$

which has the exact solution (Singh et al., 2022)

$$c(x, y, t) = \left(1 + \exp \left(\frac{1}{\sqrt{6}} \left(x - \frac{y}{\sqrt{2}} \right) - \frac{5t}{\sqrt{6}} \right) \right)^{-2}. \tag{25}$$

To validate our proposed numerical method, it is applied to the preceding problem, and we have calculated the L^2 and L^∞ normed errors between the exact and obtained numerical solutions. The results are shown through Table 1 for $n = 7, 8, 9,$ and $10, D = 0.5 = v, \lambda = 1$ at $\alpha = 0.7,$ and $\beta = 1.7.$

It is seen that L^2 and L^∞ normed errors defined by Eqs. (16) and (18) decrease as n increases. Table 1 clearly shows that the obtained numerical results by our proposed method are accurate even for small values of $n.$

For rate of convergence let us define

$$\rho_n = \frac{\|c_{n+1,n+1,n+1}(x, 1, 1) - c(x, 1, 1)\|_2}{\|c_{n,n,n}(x, 1, 1) - c(x, 1, 1)\|_2}.$$

After computation, we get $\rho_7 = 0.1716, \rho_8 = 0.1121,$ and $\rho_9 = 0.0214.$ Here $\rho_7 > \rho_8 > \rho_9$ and $\rho_7, \rho_8, \rho_9 \in (0, 1).$

Thus we get a sequence $\{\rho_n\}$ such that $\rho_n \rightarrow 0$ for sufficiently large $n.$ Hence we may conclude that the convergence of our proposed method is superlinear. Figure 2 also justifies the superlinear convergence of the method.

TABLE 1: L^2 and L^∞ errors between the approximate and the exact solutions for $n = 7, 8, 9$, and 10 for Example 1

n	$\ c(x, 1, 1) - c_{n,n,n}(x, 1, 1)\ _2$	$\ c(x, 1, 1) - c_{n,n,n}(x, 1, 1)\ _\infty$
7	1.72555×10^{-6}	1.05859×10^{-5}
8	2.96011×10^{-7}	2.53432×10^{-6}
9	3.3182×10^{-8}	9.57486×10^{-7}
10	7.1009×10^{-10}	8.32516×10^{-8}

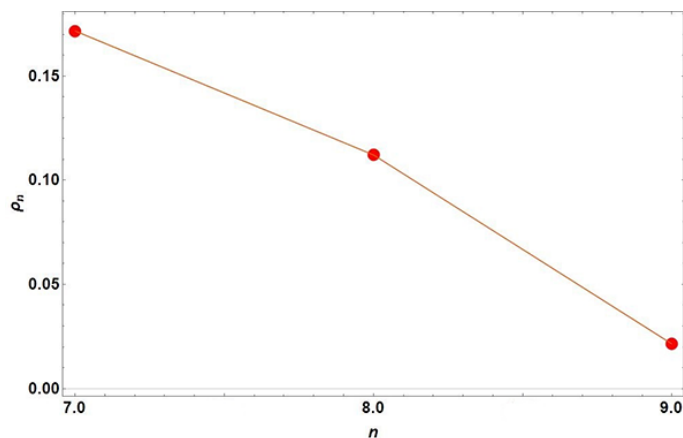


FIG. 2: Plot of rate of convergence: ρ_n against n for $n = 7, 8$, and 9 in Example 1

Example 2. The proposed method is also applied to the following problem (Pandey et al., 2021) to show its accuracy and efficiency.

$$\frac{\partial^\alpha c(x, y, t)}{\partial t^\alpha} = (0.5)(\Delta^2 c(x, y, t)) + c(x, y, t)^2(1 - c(x, y, t)) + f(x, y, t), \quad (26)$$

where

$$f(x, y, t) = e^{xy}(1.91116t^{1.1} + e^{xy}t^4(-1 + e^{xy}t^2) - 0.5t^2(x^2 + t^2)), \quad (27)$$

with initial condition

$$c(x, y, 0) = 0, \quad (28)$$

and boundary conditions

$$c(0, y, t) = t^2, \quad (29)$$

$$c(x, 0, t) = t^2, \quad (30)$$

$$c(1, y, t) = e^y t^2, \quad (31)$$

and

$$c(x, 1, t) = e^x t^2. \quad (32)$$

The exact solution is given by Pandey et al. (2021)

$$c(x, y, t) = e^{xy} t^2. \quad (33)$$

The L^2 and L^∞ normed errors between the obtained results and the exact results are calculated for $n = 6, 7, 8$, and 9, for $\alpha = 0.9$, which are displayed through Table 2. It is clear from Table 2 that our proposed numerical method is efficient even for smaller values of n .

TABLE 2: L^2 and L^∞ errors between the approximate and the exact solutions for $n = 6, 7, 8,$ and 9 for Example 2

n	$\ c(x, 1, 1) - c_{n,n,n}(x, 1, 1)\ _2$	$\ c(x, 1, 1) - c_{n,n,n}(x, 1, 1)\ _\infty$
6	3.8141×10^{-8}	4.39728×10^{-8}
7	1.17892×10^{-9}	1.2757×10^{-9}
8	3.24816×10^{-11}	1.20232×10^{-10}
9	3.6379×10^{-13}	6.12022×10^{-11}

As in the previous example, we get $\rho_6 = 0.0309, \rho_7 = 0.02755, \rho_8 = 0.01119,$ and again notice that $\rho_6 > \rho_7 > \rho_8$ and $\rho_6, \rho_7, \rho_8 \in (0, 1)$. Thus a sequence $\{\rho_n\}$ is obtained with $\rho_n \rightarrow 0$ as n becomes large, which clearly concludes that the proposed method is superlinear, which is also justified by Fig. 3.

It is also clear from Table 2 that the errors are much lower as compared to the method applied in the article (Pandey et al., 2021). Therefore, we may claim that our proposed method is superior than the existing method given in Pandey et al. (2021).

4. SOLUTION OF THE PROBLEM

After validation of the proposed numerical method on two existing problems, we employed it to solve the considered fractional-order RADE model [Eq. (1)] under the following initial condition

$$c(x, y, 0) = 1, \tag{34}$$

and boundary conditions

$$c(0, y, t) = t, \tag{35}$$

$$\frac{\partial^\beta c(1, y, t)}{\partial x^\beta} = 0, \tag{36}$$

$$\frac{\partial^\beta c(x, 0, t)}{\partial y^\beta} = 0, \tag{37}$$

$$\frac{\partial c(x, 1, t)}{\partial y} = 0. \tag{38}$$

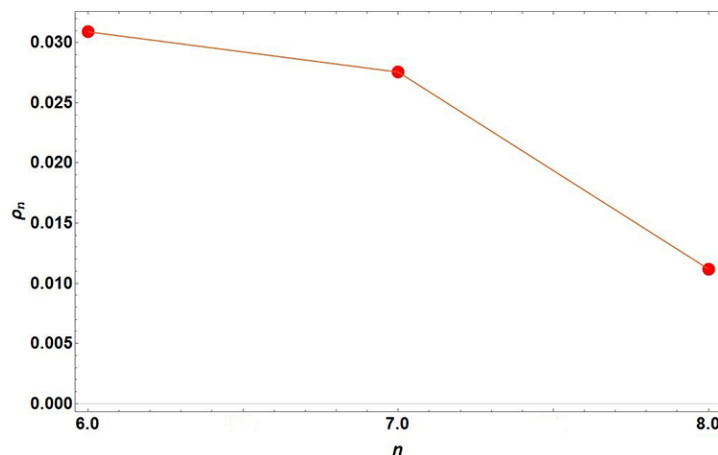


FIG. 3: Plot of rate of convergence: ρ_n against n for $n = 6, 7,$ and 8 in Example 2

To solve this model let us first approximate the unknown function $c(x, y, t)$ defined in Eq. (11) as

$$(\psi_n(t))^T C(\psi_n(x) \otimes \psi_n(y)).$$

After substituting the approximation of the unknown function $c(x, y, t)$ and using an operational matrix of the fractional-order derivative defined in Eq. (12), and taking everything on the left-hand side and adding the initial condition to this resulting equation, we get

$$\begin{aligned} & (\psi_n(t))^T (D^{(\alpha)})C(\psi_n(x) \otimes \psi_n(y)) - D(\psi_n(t))^T C(D^{(2\beta)} \otimes I)(\psi_n(x) \otimes \psi_n(y)) \\ & - D(\psi_n(t))^T C(I \otimes D^{(2\beta)})(\psi_n(x) \otimes \psi_n(y)) \\ & + \nu_1(\psi_n(t))^T C(D^{(\beta)} \otimes I)(\psi_n(x) \otimes \psi_n(y)) \\ & + \nu_2(\psi_n(t))^T C(I \otimes D^{(\beta)})(\psi_n(x) \otimes \psi_n(y)) \\ & + \lambda(\psi_n(t))^T C(\psi_n(x) \otimes \psi_n(y))(1 - (\psi_n(t))^T C(\psi_n(x) \otimes \psi_n(y))) = 0, \end{aligned} \quad (39)$$

and the approximation of the boundary conditions are given by

$$(\psi_n(t))^T C(\psi_n(0) \otimes \psi_n(y)) - t = 0, \quad (40)$$

$$(\psi_n(t))^T C(D_n^{(\beta)} \otimes I)(\psi_n(1) \otimes \psi_n(y)) = 0, \quad (41)$$

$$(\psi_n(t))^T C(I \otimes D_n^{(\beta)})(\psi_n(x) \otimes \psi_n(0)) = 0, \quad (42)$$

$$(\psi_n(t))^T C(I \otimes D_n^{(1)})(\psi_n(x) \otimes \psi_n(1)) = 0. \quad (43)$$

We will now collocate the Eq. (39) at points (x_i, y_j, t_k) and Eqs. (40) to (43) at points (x_i, t_k) and at points (y_j, t_k) , where x_i, y_j are Legendre–Gauss–Lobatto (LGL) points of the $L_{n-1}(x)$ and $L_{n-1}(y)$, respectively, where t_k are the zeroes of the shifted Legendre polynomial $L_{n+1}(t)$. After the collocation, the equations are converted to a linear system of algebraic equations from which the unknown matrix C can be obtained by using the Newton method. Substituting the matrix C , the approximate solution of $c(x, y, t)$ will be obtained.

Figure 4 depicts the movement of solute concentration due to variations of $\beta = 0.7, 0.8, 0.9,$ and 1.0 at fixed $t = 1$ and $\alpha = 0.8$, while Fig. 5 represents the movement of solute concentration due to variations of $\beta = 0.7, 0.8, 0.9,$ and 1.0 at fixed $t = 1$ and $\alpha = 0.9$, and Fig. 6 represents the movement of solute concentration for $\beta = 0.7, 0.8, 0.9,$ and 1.0 at fixed $t = 1$ and $\alpha = 1.0$. Hence from Figs. 4, 5, and 6, we observe that for a fixed α the concentration of solution increases as β varies from integer order to fractional order. In each case it is found that as β (the order of spatial derivative) decreases, the solute concentration increases.

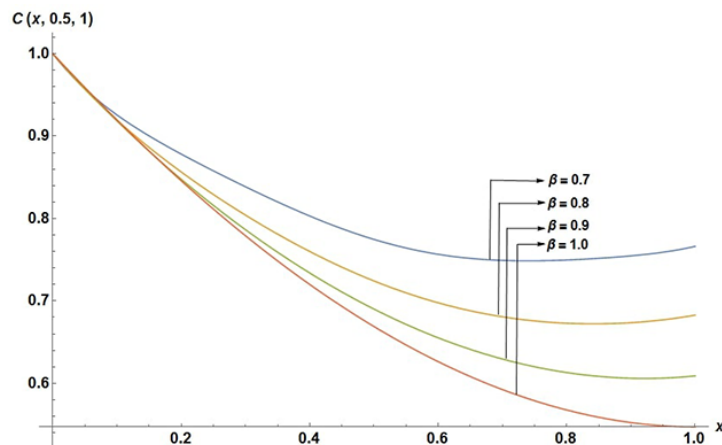


FIG. 4: Plots of solute concentration at fixed $t = 1$ for $\alpha = 0.8$ and $\beta = 0.7, 0.8, 0.9,$ and 1.0

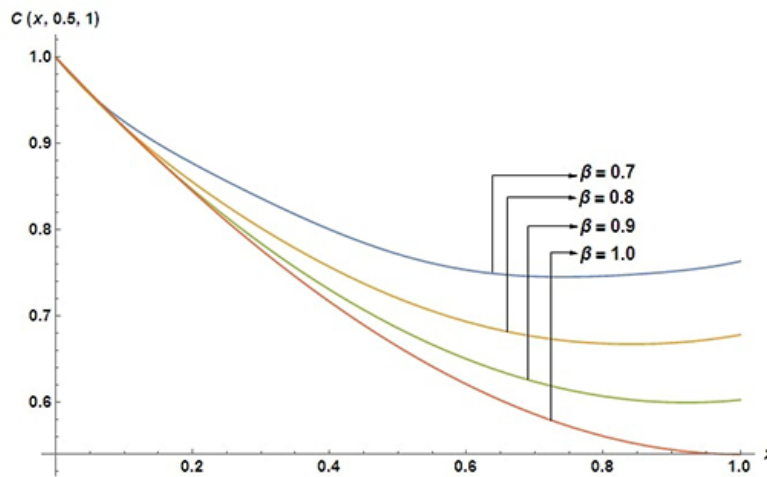


FIG. 5: Plots of solute concentration at fixed $t = 1$ for $\alpha = 0.9$ and $\beta = 0.7, 0.8, 0.9,$ and 1.0

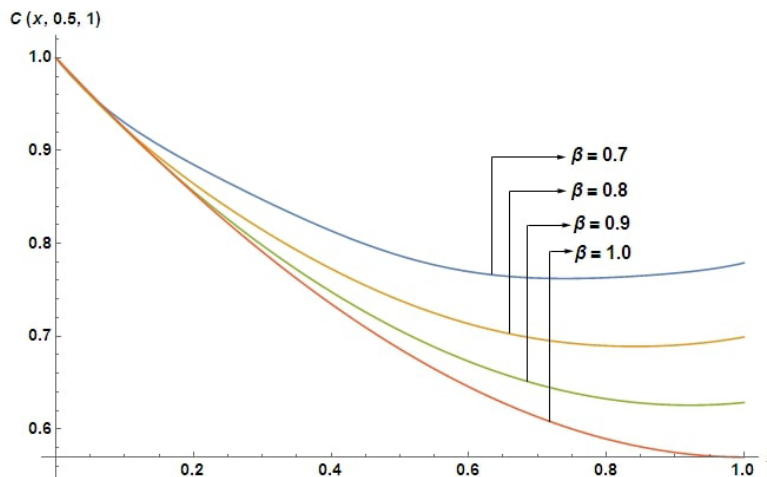


FIG. 6: Plots of solute concentration at fixed $t = 1$ for $\alpha = 1.0$ and $\beta = 0.7, 0.8, 0.9,$ and 1.0

Figure 7 is the plot of the movement of solute concentration for $\alpha = 0.8, 0.9,$ and 1.0 at fixed $t = 1$ and $\beta = 1.0$. Hence we can observe that for a fixed $\beta = 1.0$, the solute concentration decreases as α varies from integer order to fractional order. These results demonstrate not only the role of the order of the derivatives in describing effectively the pollutant transport in porous media but also the need to employ the FRADE instead of RADE to study the fate of pollutant transportation in such systems.

Figure 8 shows the variations of solute concentration at $\beta = 0.8 = \alpha, \nu_1 = 0.3, \nu_2 = 0.6, D = 1,$ and $t = 1$ for the values $\lambda = -1, 0,$ and 1 . Figure 9 represents the variation of solute concentration at $\beta = 0.8 = \alpha, \nu_1 = 0.6, \nu_2 = 0.3, D = 1, t = 1$ for $\lambda = -1, 0,$ and 1 . Figure 10 represents the plot of solute concentration at $\beta = 1.0 = \alpha, \nu_1 = 0.3, \nu_2 = 0.6, D = 1, t = 1$ for $\lambda = -1, 0,$ and 1 . Figure 11 represents the plot of solute concentration at $\beta = 1.0 = \alpha, \nu_1 = 0.6, \nu_2 = 0.3, D = 1, t = 1$ for $\lambda = -1, 0,$ and 1 . Hence from Figs. 8, 9, 10, and 11, we can observe that for a fixed value of α and β , the solute concentration is less for the system with sink term ($\lambda = 1$), as compared to the system with conservative contaminant ($\lambda = 0$) and for the system with source term ($\lambda = -1$). This is physically justified that more damping will be found in the presence of the sink term ($\lambda = 1$) as compared to the source term ($\lambda = -1$) as well as for the case of conservative system ($\lambda = 0$).

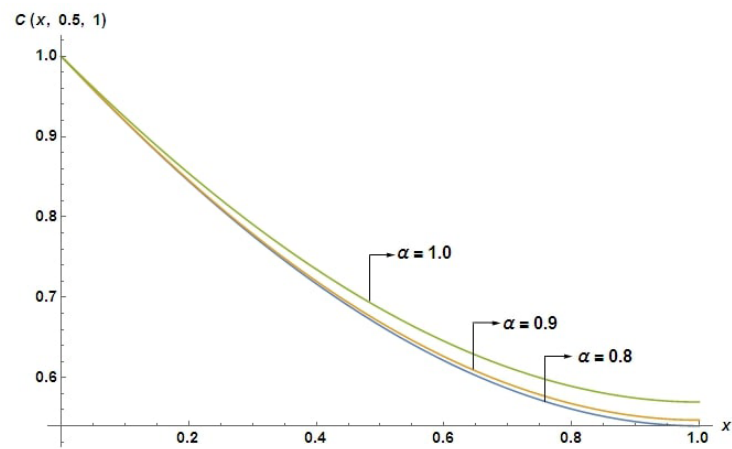


FIG. 7: Plots of concentration of solution at fixed $t = 1$ for $\beta = 1.0$ and $\alpha = 0.8, 0.9$, and 1.0

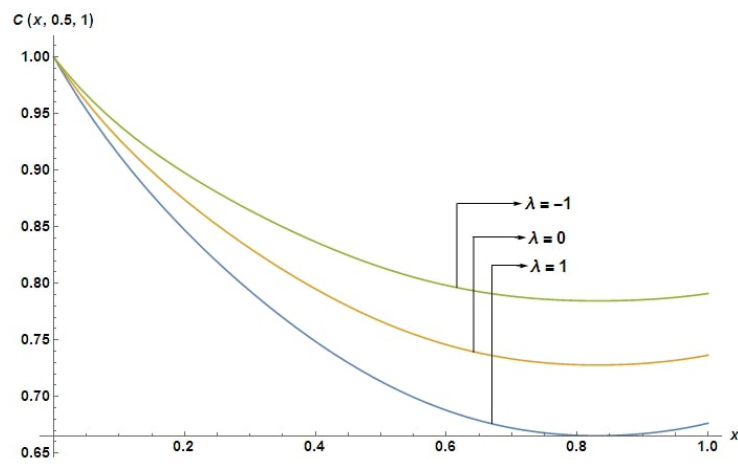


FIG. 8: Plots of concentration of solution at fixed $t = 1$ for $\alpha = 0.8 = \beta$, $\nu_1 = 0.3$, $\nu_2 = 0.6$, $D = 1$, and $\lambda = -1, 0$, and 1

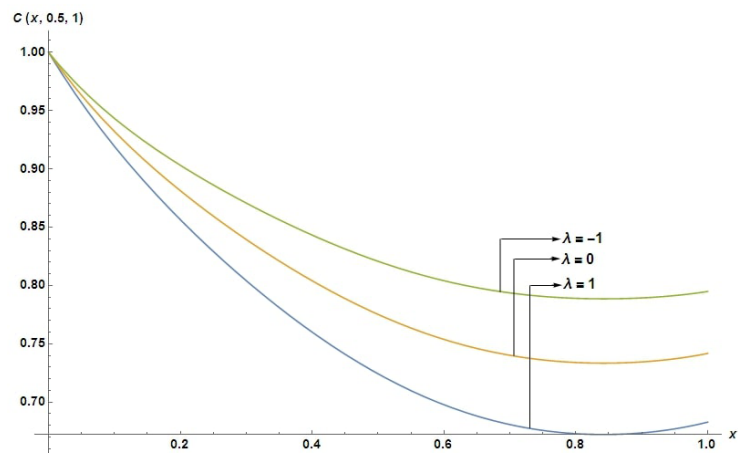


FIG. 9: Plots of solute concentration at fixed $t = 1$ for $\alpha = 0.8 = \beta$, $\nu_1 = 0.6$, $\nu_2 = 0.3$, $D = 1$, and $\lambda = -1, 0$, and 1

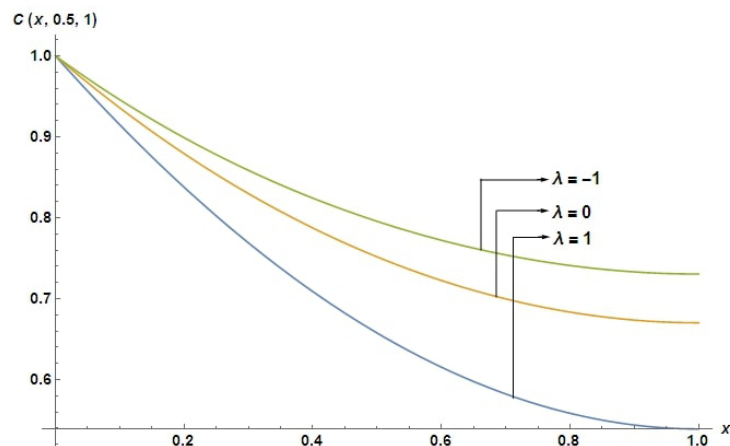


FIG. 10: Plots of solute concentration at fixed $t = 1$ for $\alpha = 1.0 = \beta$, $\nu_1 = 0.3$, $\nu_2 = 0.6$, $D = 1$, and $\lambda = -1, 0$, and 1

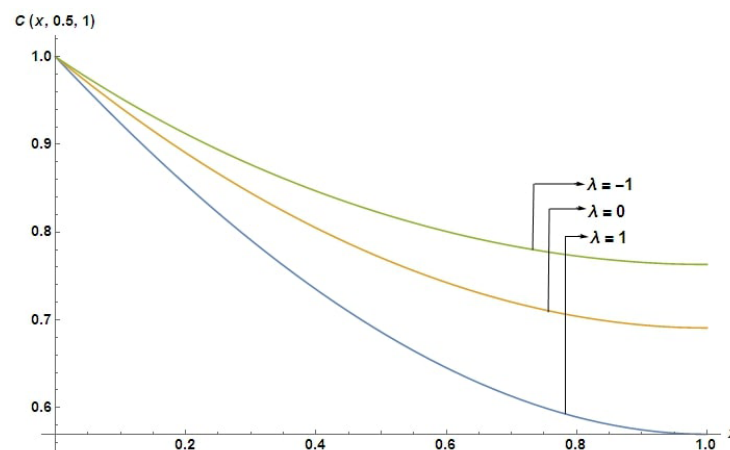


FIG. 11: Plots of solute concentration at fixed $t = 1$ for $\alpha = 1.0 = \beta$, $\nu_1 = 0.6$, $\nu_2 = 0.3$, $D = 1$, and $\lambda = -1, 0$, and 1

5. CONCLUSION

In the present scientific contribution the nonlinear space-time fractional-order RADE problem is solved by using a numerical method known as the shifted Legendre collocation method with the help of the operational matrices for derivatives. The accuracy and efficiency of the method are confirmed through error analyses of the results obtained between the proposed approach and the existing analytical method. Then, the proposed methodology is employed to solve the contaminant transport in a groundwater problem defined by FRADE. For variations in space and time, the effect caused by the advection term on the solution profile is visually shown along with the impact of order of the spatial and time derivatives on the solution profile. Another focus of the research is the explanation of the damping of the solution profile as the system approaches to fractional order from standard order. The authors believe that the current contribution will be useful to scientists and engineers working in the field of transport in porous media.

ACKNOWLEDGMENTS

The authors would like to thank the reviewers for their constructive comments and suggestions to improve the quality of the revised article. The authors acknowledge the project grant provided by Board of Research in Nuclear Sciences (BRNS), BARC, Government of India (Sanction No. 58/14/07/2022-BRNS).

REFERENCES

- Ahmed, S.E. and Rashed, Z., 3D Buoyancy-Driven Flow within Cubic Enclosures Filled with Hydrodynamically and Thermally Heterogeneous Porous Media Using Non-Homogeneous Nanofluid Model, *J. Porous Media*, vol. **24**, no. 11, pp. 13–75, 2021.
- Atangana, A. and Baleanu, D., Caputo-Fabrizio Derivative Applied to Groundwater Flow within Confined Aquifer, *J. Eng. Mech.*, vol. **143**, no. 5, Article ID D4016005, 2017.
- Benson, D.A., Wheatcraft, S.W., and Meerschaert, M.M., Application of a Fractional Advection-Dispersion Equation, *Water Resour. Res.*, vol. **36**, no. 6, pp. 1403–1412, 2000a.
- Benson, D.A., Wheatcraft, S.W., and Meerschaert, M.M., The Fractional-Order Governing Equation of Lévy Motion, *Water Resour. Res.*, vol. **36**, no. 6, pp. 1413–1423, 2000b.
- Bhrawy, A. and Baleanu, D., A Spectral Legendre–Gauss–Lobatto Collocation Method for a Space-Fractional Advection Diffusion Equations with Variable Coefficients, *Rep. Math. Phys.*, vol. **72**, no. 2, pp. 219–233, 2013.
- Brewer, J., Kronecker Products and Matrix Calculus in System Theory, *IEEE Trans. Circuits Syst.*, vol. **25**, no. 9, pp. 772–781, 1978.
- Chen, Y., Wu, Y., Cui, Y., Wang, Z., and Jin, D., Wavelet Method for a Class of Fractional Convection-Diffusion Equation with Variable Coefficients, *J. Comput. Sci.*, vol. **1**, no. 3, pp. 146–149, 2010.
- Cui, M., Compact Exponential Scheme for the Time Fractional Convection–Diffusion Reaction Equation with Variable Coefficients, *J. Comput. Phys.*, vol. **280**, pp. 143–163, 2015.
- Das, S., Analytical Solution of a Fractional Diffusion Equation by Variational Iteration Method, *Comput. Math. Appl.*, vol. **57**, no. 3, pp. 483–487, 2009.
- Das, S., Kumar, V., and Gupta, P.K., Solution of the Nonlinear Fractional Diffusion Equation with Absorbent Term and External Force, *Appl. Math. Model.*, vol. **35**, no. 8, pp. 3970–3979, 2011.
- Davarzani, H., Marcoux, M., and Quintard, M., A Local Thermal Nonequilibrium Model for Coupled Heat and Mass Transfer with Dispersion and Thermal Diffusion, in *Porous Media*, *J. Porous Media*, vol. **24**, no. 11, pp. 37–63, 2021.
- Del-Castillo-Negrete, D., Carreras, B., and Lynch, V., Nondiffusive Transport in Plasma Turbulence: A Fractional Diffusion Approach, *Phys. Rev. Lett.*, vol. **94**, no. 6, Article ID 065003, 2005.
- El-Amin, M.F., Derivation of Fractional-Derivative Models of Multiphase Fluid Flows in Porous Media, *J. King Saud Univ. Sci.*, vol. **33**, no. 2, Article ID 101346, 2021.
- Gerolymatou, E., Vardoulakis, I., and Hilfer, R., Modelling Infiltration by Means of a Nonlinear Fractional Diffusion Model, *J. Phys. D: Appl. Phys.*, vol. **39**, no. 18, Article ID 4104, 2006.
- Ghazal, M. and Behrouz, M., Modelling Solute Transport in Homogeneous and Heterogeneous Porous Media Using Spatial Fractional Advection-Dispersion Equation, *Soil Water Res.*, vol. **13**, no. 1, pp. 18–28, 2018.
- Jaiswal, S., Chopra, M., and Das, S., Numerical Solution of a Space Fractional Order Solute Transport System, *J. Porous Media*, vol. **21**, no. 2, pp. 145–160, 2018.
- Karapanagioti, H.K., Gossard, C.M., Strevett, K.A., Kolar, R.L., and Sabatini, D.A., Model Coupling Intraparticle Diffusion/sorption, Nonlinear Sorption, and Biodegradation Processes, *J. Contaminant Hydrol.*, vol. **48**, nos. 1-2, pp. 1–21, 2001.
- Lee, S., Lee, S., and Choi, J., Nonlinear Sorption of Organic Contaminant during Two-Dimensional Transport in Saturated Sand, *Water*, vol. **13**, no. 11, Article ID 1557, 2021.
- Ngondiep, E., A Two-Level Fourth-Order Approach for Time-Fractional Convection–Diffusion–Reaction Equation with Variable Coefficients, *Commun. Nonlinear Sci. Numer. Simul.*, vol. **111**, Article ID 106444, 2022.
- Pandey, P., Das, S., Craciun, E., and Sadowski, T., Two-Dimensional Nonlinear Time Fractional Reaction–Diffusion Equation in Application to Sub-Diffusion Process of the Multicomponent Fluid in Porous Media, *Meccanica*, vol. **56**, no. 1, pp. 99–115, 2021.
- Plociniczak, Ł., Analytical Studies of a Time-Fractional Porous Medium Equation. Derivation, Approximation and Applications, *Commun. Nonlinear Sci. Numer. Simul.*, vol. **24**, nos. 1-3, pp. 169–183, 2015.
- Qawasmeh, B.R., Duwairi, H.M., and Alrbai, M., Non-Darcian Forced Convection Heat Transfer of Williamson Fluid in Porous Media, *J. Porous Media*, vol. **24**, no. 8, pp. 23–35, 2021.
- Saadatmandi, A. and Dehghan, M., A New Operational Matrix for Solving Fractional-Order Differential Equations, *Comput. Math.*

- Appl.*, vol. **59**, no. 3, pp. 1326–1336, 2010.
- Sayevand, K., Machado, J.T., and Masti, I., Analysis of Dual Bernstein Operators in the Solution of the Fractional Convection–Diffusion Equation Arising in Underground Water Pollution, *J. Comput. Appl. Math.*, vol. **399**, Article ID 113729, 2022.
- Singh, A. and Das, S., Study and Analysis of Spatial-Time Nonlinear Fractional-Order Reaction-Advection-Diffusion Equation, *J. Porous Media*, vol. **22**, no. 7, pp. 787–798, 2019.
- Singh, A., Das, S., and Ong, S., Study and Analysis of Nonlinear (2+1)-Dimensional Solute Transport Equation in Porous Media, *Math. Comput. Simul.*, vol. **192**, pp. 491–500, 2022.
- Singh, A., Das, S., Ong, S.H., and Jafari, H., Numerical Solution of Nonlinear Reaction–Advection–Diffusion Equation, *J. Comput. Nonlinear Dyn.*, vol. **14**, no. 4, Article ID 041003, 2019.
- Sohail, A., Kashif, A., and Muhammad, A., MHD Flow of Cu–Al₂O₃/Water Hybrid Nanofluid through a Porous Media, *J. Porous Media*, vol. **24**, no. 7, pp. 61–73, 2021.
- Tarasov, V.E., Transport Equations from Liouville Equations for Fractional Systems, *Int. J. Modern Phys. B*, vol. **20**, no. 3, pp. 341–353, 2006.
- Wang, Z., Guo, J., Pan, Z., Qiao, L., Liu, J., and Li, W., A Generalized Matrix-Fracture Flow Transfer Model for Fracture Porous Media, *J. Porous Media*, vol. **24**, no. 3, pp. 51–75, 2021.
- Zhang, H. and Ding, F., On the Kronecker Products and Their Applications, *J. Appl. Math.*, vol. **2013**, Article ID 296185, 2013.
- Zhou, H. and Yang, S., Fractional Derivative Approach to Non-Darcian Flow in Porous Media, *J. Hydrol.*, vol. **566**, pp. 910–918, 2018.